Hindawi
International Journal of Aerospace Engineering
Volume 2023, Article ID 2155528, 12 pages
https://doi.org/10.1155/2023/2155528

Research Article

A Comparative Research of Control System Design Based on H-Infinity and ALQR for the Liquid Rocket Engine of Variable Thrust

Fayin Chen,[1] **Wei Xue**,[2] **Yong Tang**,[3,4] **and Tao Wang**[1,5]

[1]*School of Intelligent Systems Engineering, Sun Yat-Sen University, Guangzhou 510006, China*
[2]*China Academy of Aerospace Science and Innovation, Beijing 100076, China*
[3]*School of Civil Aviation, Northwestern Polytechnical University, Xi'an, 710072, China*
[4]*UAS Co., Ltd., Aviation Industry Corporation of China (Chengdu), Chengdu 610097, China*
[5]*Southern Marine Science and Engineering Guangdong Laboratory (Zhuhai), Zhuhai, Guangdong 519000, China*

Correspondence should be addressed to Tao Wang; wangt339@mail.sysu.edu.cn

Received 10 September 2022; Accepted 24 February 2023; Published 23 March 2023

Academic Editor: Erkan Kayacan

The design and analysis procedures for the thrust controller used in variable-thrust rocket engines are substantially different from those used in conventional engines due to the large-scale thrust adjustment capabilities that result in a wide range of operating situations. In this study, two control algorithms, h-infinity and adaptive linear quadratic regulator (ALQR), are constructed, examined, and contrasted utilizing the adaptive control system architecture. Both methods are capable of producing engines that respond in less than one second, have a steady-state error of less than two percent, and are robust.

1. Introduction

Due to its capacity to regulate thrust, the variable-thrust liquid rocket engine has numerous technical advantages as an aeronautical power source. Variable-thrust liquid rocket engines can alter their thrust in a wide range and under complicated operating conditions when compared to fixed-thrust rocket engines. As we all known, variable-thrust liquid rocket engine is the novel challenging topic for the related researchers and engineers. This paper mainly focuses on the control system design methods for variable-thrust rocket engines, which can be used for the reconfigurations of the flight control models. Since its control system design must be more robust, there are notable variations in the analysis and design processes. Tracking the combustion chamber pressure is the primary control challenge of a variable-thrust liquid rocket engine, which can be accomplished by adjusting the flow control valve [1]. The aim of managing the thrust by altering the pressure in the combustion chamber is accomplished, and a review of various control systems reveals that the PID method is used by the majority of them. The traditional PID algorithm struggles to deal with the complex working conditions generated by the variable-thrust engine's continuous operation, as well as the structural disturbances that will be generated during the engine operation. This paper's adaptive framework and robust algorithm can effectively improve the overall robustness of the control process, cope with drastic changes in the engine's working environment, and serve as a reference algorithm design for reusable variable-thrust engines.

Solenoid valve hydraulic control technology is heavily utilized in the thrust control system of variable-thrust liquid rocket engines [2, 3]. It is feasible to regulate the thrust system of these engines by altering the control valves in the combustion chambers [4, 5]. The three main loops that are required for the proper operation of variable-thrust liquid rocket engines are thrust control, propellant usage control,

and thrust vector control [6]. These loops and subsystems are in charge of gathering sensor data and changing the controllable inputs to determine the state of the engine and process variables. Based on the aforementioned techniques that use an open loop to achieve thrust control, Pérez-Roca et al., Xin et al., Yun-qin, Bellows et al., Le Gonidec, Huzel and Huang, Timnat, Lorenzo and Musgrave, Sutton and Biblarz, Dai and Ray, and Kiforenko and Kharitonov developed an open-loop optimal control strategy in [1–11] for controlling the thrust of a rocket engine. However, the majority of investigations employ closed-loop control. They often choose for the traditional PID-based strategy to control the engine's linearized model [12–15]. Le Gonidec and Faye incorporate nonlinearity into the control technique to avoid overtaxing the engine [16]. There is also literature on filtering the input set signal by including a filter module [17]. Reactions to specific faults and uncertainties are a feature of several approaches [18, 19] that improve the engine control system's robustness.

A liquid rocket engine's operation involves a number of unclear characteristics that could vary from operation to operation. In this study, a control system is presented, whereby the controller settings are altered to adapt to the engine operating conditions. A robust algorithm is used to change these values, and using robust control techniques can significantly increase system stability [20]. ALQR and h-infinity are two distinct robust algorithms that are employed. The h-infinity control theory is a powerful approach for dealing with the uncertainty of the model [20, 21]. It uses the infinite norm of the system transfer function as the optimum design index in Hardy space to arrive at a robust control theory [22, 23]. Augmented Linear Quadratic Optimal Control (ALQR) may eliminate steady-state errors and offers an unlimited amplitude margin and phase angle margin of more than 60° [24–26].

Control methods may adapt to changing operational conditions and upsetting effects and are employed in a wide range of control applications [27–30]. In this study, the engine control system is designed using the hybrid sensitivity function, a typical h-infinity method problem [31]. The noise may be successfully muted and response time can be increased with the controller's design. The variable-thrust liquid rocket engine is subjected to the augmented LQR approach using the derivatives of the original system state and the command error as augmented state vectors. It satisfies the control needs of aeroengine command tracking in addition to having good robustness.

The features of variable-thrust liquid rocket engines, the need for liquid rocket engine control, and the nature and characteristics of two robust control systems are all briefly covered in the first half of the paper. In the second section, the variable-thrust liquid rocket engine's system concept is presented. Additionally, a mathematical model of the engine created using the system identification approach is provided. In Section III, the engine control issue is examined, the two control approaches are integrated into the adaptive framework for engine thrust control, and MATLAB and Simulink are used to simulate and analyze the entire system. The two control strategies are outlined and contrasted in Section IV when they are used with a variable-thrust liquid rocket engine.

2. Model of the Liquid Rocket Engine

Rocket engines do not require outside air; instead, power is directly produced by the internal combustion of propellants and is then ejected at high speed to produce thrust. In contrast, aeroengines require the inhalation of air, which is burned and compressed before being ejected at high speed to produce thrust. Aerospace technology's variable-thrust liquid rocket engines have dual-adjustable injectors and cavitation ventilators, which enable a wide range of operating conditions and great performance. The design provides good atomization, guarantees combustion stability, and boosts combustion efficiency. It also maintains the appropriate propellant component ratio throughout the operating circumstances. Simple moving components that are simple to modify and guarantee dependable operation are found in the injectors and venturi.

A schematic diagram of a liquid rocket motor system is shown in Figure 1. Pulse width modulation technologies, such as solenoid valves and hydraulic actuators, are used as actuators in liquid rocket engines with variable thrust. The rocket motor's flow regulation is controlled by a solenoid-hydraulic valve actuation system. The input and output solenoid valves are operated to operate in various operating modes by sending control signals from the solenoid valves. The hydraulic system then drives the actuator, altering the venturi's regulating cone's stroke. The controlled flow and the opening stroke of the regulating cone are linearly correlated in the linearly adjustable cavitation venturi [32]. Therefore, it is possible to control the flow of the oxidizer and combustion agent in order to achieve the goal of managing the pressure in the combustion chamber by controlling the time at which the solenoid valves at the intake and exit open.

As described above, there is a complex process of mechanical motion and chemical reaction between the actuator motion and the combustion chamber pressure output of the rocket motor. Due to the limitation of real-time data acquisition, it is therefore difficult to obtain the theoretical modeling of the rocket motor flow and injector through the analysis of the mechanism. Considering all aspects, this paper adopts the mathematical model of the rocket engine established by the system identification method. The selected actuator displacement is used as the input $r(t)$, which determines the lift of the venturi regulating cone, while the pressure in the combustion chamber is used as the output $y(t)$, and the least squares method is used for parameter identification to obtain the mathematical model of the system.

Since the dynamic characteristics of the engine chamber pressure change during both rise and fall, and the characteristics change significantly under different operating conditions, it is difficult for the linear mathematical model with fixed parameters to describe the dynamic characteristics of the engine under all conditions more accurately, and the engine has high requirements for control performance and

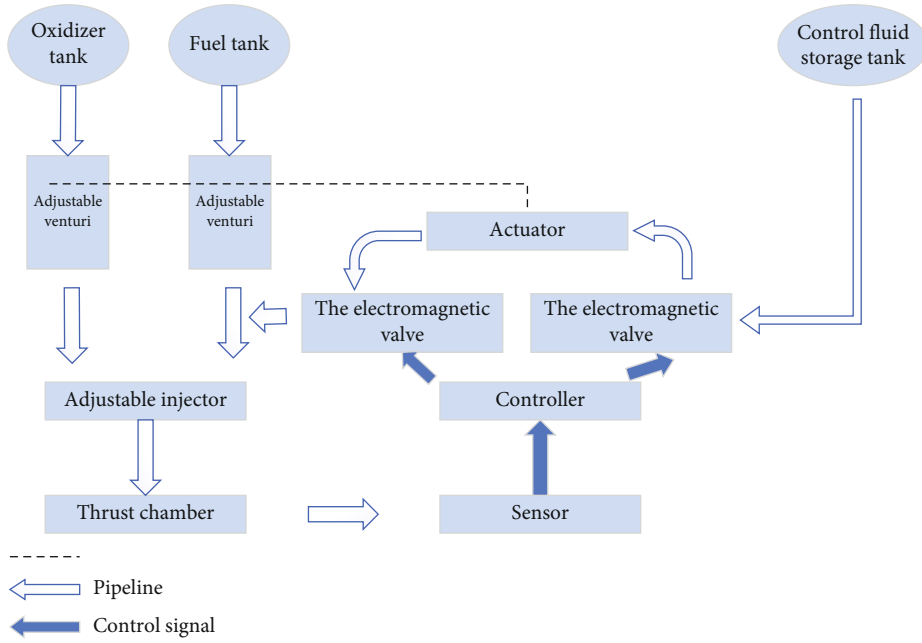

Figure 1: A scheme of variable-thrust liquid rocket engine control system.

stability. Therefore, after determining the engine models under different operating conditions, the model in this paper uses different parameter models to describe them according to different chamber pressures and operating conditions, so that the simulation is closer to reality. Based on the cold test data, the data of the engine system under different operating conditions are identified and the corresponding transfer functions are obtained [33]. The model is then stimulated with the raw input data to obtain the model output, which is compared with the raw output data. The similarity between the model output and the actual output is described using the goodness-of-fit.

$$\text{Fit} = 1 - \frac{\sum \hat{y}_k - y_k{}^2}{\sum (y_k - \bar{y})^2}. \tag{1}$$

y_k represents the actual output value at the kth sampling time, $\hat{y}_k$ represents the model output value at the kth sampling time, and $\bar{y}$ represents the average value of the actual output. The closer the degree of fit is to 1, the closer the system described by the model is to reality.

The fit of the different order models is listed in Table 1. It can be observed that the order of the model should not be less than the 2 orders, and the fitting degrees of the model after the 3 orders are not improved much, so the model order should be 2 or 3 orders.

The engine models identified by cold test and hot test data under different operating conditions are given below [34];

The cold test rising condition (from high condition to low condition) is as follows:

$$\frac{231.7s^2 - 5.375e005s + 4.796e008}{s^3 + 1139s^2 + 1.021e006s + 4.44e008}, \tag{2}$$

Table 1: Temperature and wildlife count in the three areas covered by the study.

Model order (denominator orders molecular orders)	Fit
(1 1)	0.7208
(2 1)	0.8021
(2 2)	0.7983
(3 1)	0.9443
(3 2)	0.9437
(3 3)	0.9456
(4 1)	0.9807
(4 2)	0.9719
(4 3)	0.9839
(4 4)	0.9853

$$\frac{283.3s^2 - 6.492e005s + 5.959e008}{s^3 + 1285s^2 + 9.229e005s + 4.929e008}, \tag{3}$$

$$\frac{185.4s^2 - 4.593e005s + 4.368e008}{s^3 + 740.7s^2 + 9.449e005s + 3.386e008}, \tag{4}$$

$$\frac{147.4s^2 - 3.681e005s + 3.511e008}{s^3 + 667.4s^2 + 9.945e005s + 2.601e008}. \tag{5}$$

The cold test down condition (from high condition to low condition) is as follows:

$$\frac{534.7s^2 - 1.222e006s + 1.147e009}{s^3 + 1134s^2 + 1.164e006s + 8.183e008}, \tag{6}$$

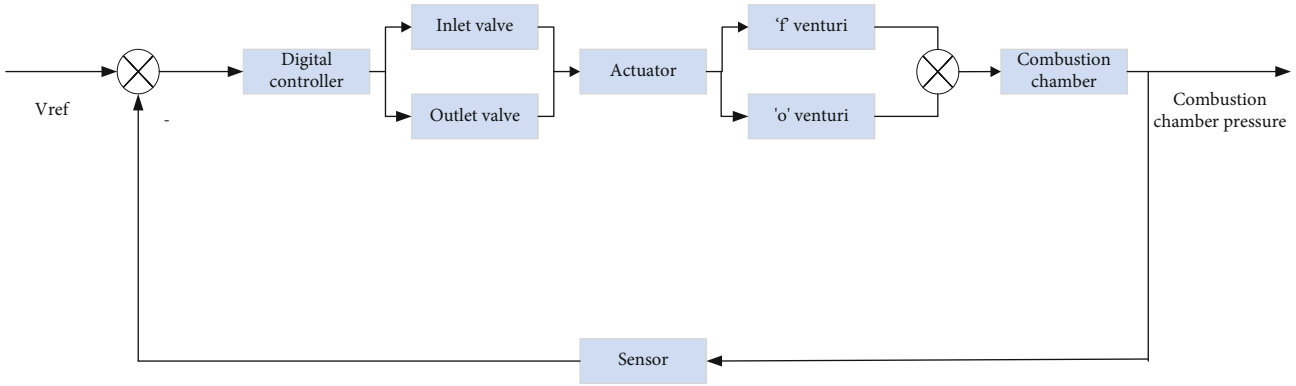

Figure 2: Control system structure diagram.

$$\frac{135.3s^2 - 3.151e005s + 2.855e008}{s^3 + 1386s^2 + 5.832e005s + 2.985e008}, \tag{7}$$

$$\frac{100s^2 - 2.584e005s + 2.45e008}{s^3 + 717.6s^2 + 4.791e005s + 1.726e008}. \tag{8}$$

The hot test rising working conditions (from high working conditions to low working conditions) are as follows:

$$\frac{17.94s^2 - 8.79e004s + 1.644e008}{s^3 + 1770s^2 + 3.335e006s + 1.329e009}, \tag{9}$$

$$\frac{22.86s^2 - 1.153e005s + 2.719e008}{s^3 + 1537s^2 + 2.719e006s + 1.547e009}. \tag{10}$$

The hot test down working conditions (from high working conditions to low working conditions) are as follows:

$$\frac{5.662s^2 - 2.932e004s + 5.523e007}{s^3 + 1509s^2 + 1.533e006s + 3.806e008}. \tag{11}$$

2.1. Controller Design for Liquid Rocket Engine. As a control object, the variable-thrust liquid rocket engine has large parameter variations under different operating conditions. Conventional control algorithms cannot solve this problem well, but adaptive control methods are a suitable approach. An adaptive system is a system with some adaptability. It can sense changes and automatically correct the control parameters when the operative conditions change, so the system still has the adaptive control effect.

At present, solenoid valve hydraulic control technology has been widely used in variable-thrust liquid engine systems. The engine control system used in this paper is shown in Figure 2. The system adopts a single closed-loop structure, and the combustion chamber pressure is used as the control variable. The hydraulic actuator as actuator converts the acting on the solenoid valve into the displacement of the actuator piston and drives the flow-regulating element on the engine to adjust the flow of the combustion agent and the oxidant, thereby controlling the pressure of the combustion chamber.

Self-tuning control belongs to the adaptive control method, which is used according to the different operating conditions of the variable-thrust engine system and the different nature of the system model parameters. The controller corresponding to each operating condition is set, the same controller is used for similar operating conditions, and the system is matched with different controllers according to the different operating conditions.

The necessary controller parameters are designed based on models of various working scenarios, as illustrated in Figure 3. The output value of the combustion chamber pressure returned by sampling is compared to the sample chamber pressure, and the difference value is compared to the step height between working conditions in order to determine the proportional coefficient. To decide whether to modify the controller's parameters, the proportional coefficient is utilized as the reference value for the adjustment amount. Examples of unknown disturbances include unexpected engine failures brought on by structural damage and component deformation, whereas recognized disturbances include combustion instabilities at low and high frequencies [35]. The h-infinity approach is reliable and efficient for suppressing these disturbances.

2.2. H-Infinity Mixed Sensitivity Design

2.2.1. H-Infinity Control Strategy. H-infinite optimal control is the use of h-infinite parametrization as a measure of the objective function to optimize the design of the system. The h-infinite parametrization is a parametrization defined on Hardy space. In h-infinite control theory, it refers to the maximum singular value of the matrix of rational functions analyzed on the right half-plane of s. In the case of scalar functions, it refers to the maximum value of the amplitude-frequency characteristic [32]. Thus, the effect of a disturbance with a minimum power spectrum on the system can be minimized if the h-infinity parametrization of the transfer function from the system disturbance to the error is minimized. This is the basic idea of infinite control.

The main idea of the mixed sensitivity method is to select the weighted matrix W_1, W_2, W_3 in the frequency domain to meet the multiobjective requirements of the closed-loop system design, transform the control object into the state space expression of the generalized controlled object with mixed sensitivity, and solve the mixed sensitivity problem in the time domain. The h-infinity norm of a

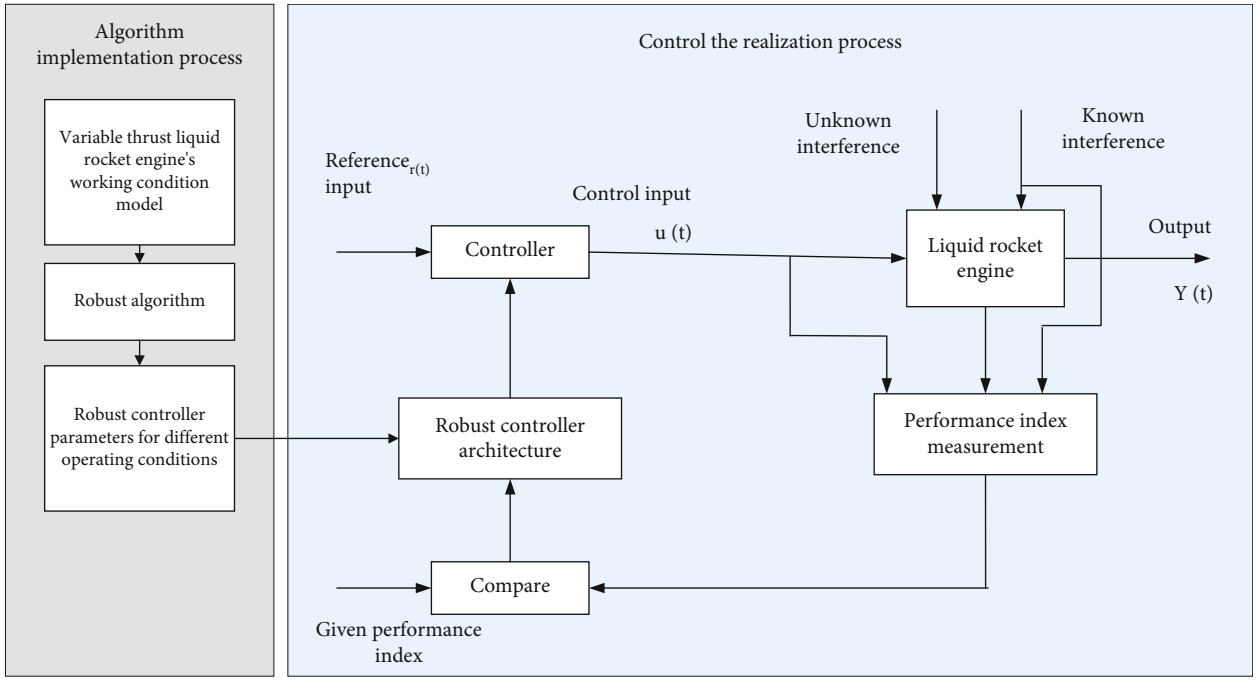

Figure 3: Schematic diagram of the adaptive control system.

function matrix is defined as [36]

$$\|T(s)\|_{\infty} = \sup_{k \in R} \bar{e}[T(jk)]. \tag{12}$$

The tracking problem for a linear time-invariant system is shown in Figure 4 where r, e, u, d, y are the reference input, tracking error, input control, measured disturbance, and thrust output, respectively, K is the controller, and G is the engine mathematical model. Assuming $G(\infty) = 0$, the transfer functions of r to e and u and y are

$$S = (I + GK)^{-1}, \tag{13}$$

$$R_h = K(I + GK)^{-1} = KS, \tag{14}$$

$$T = GK(I + GK)^{-1} = I - S. \tag{15}$$

where S and T are called the sensitivity function and complementary sensitivity function. The smaller the gain of S, the smaller the tracking error of the corresponding system and the better the response of the obtained system. The complementary sensitivity function T is an important indicator to determine the robust stability of the system, and the effect of model uncertainty on the system can be suppressed by reducing the magnitude of T. However, it can be seen from Equation (15) that both S and T indicators cannot be reduced at the same time. In general, most of the interfering signals are low-frequency signals and the system uncertainty appears in the high-frequency band, so the trade-off between the two indicators should be made according to the actual situation in choosing the weighting function. In contrast, the split-condition rocket engine model

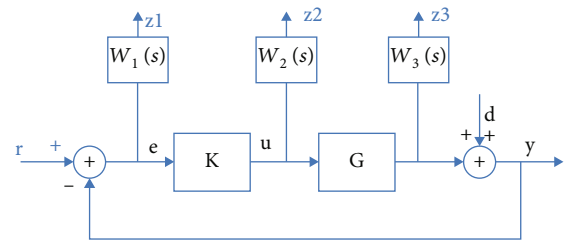

Figure 4: Block diagram of mixed sensitivity control.

used in this paper has been modeled by identifying the operating conditions to properly reduce the system uncertainty.

As shown in Figure 4, the transfer functions of interference d to z_1, z_2, and z_3 are W_1S, W_2R, and W_3T, respectively. The framework of the mixed sensitivity problem is

$$\begin{bmatrix} W_1 e \\ W_2 u \\ W_3 y \\ e \end{bmatrix} = \begin{bmatrix} W_1 & -W_1 G \\ 0 & W_2 \\ 0 & W_3 G \\ I & -G \end{bmatrix} \begin{bmatrix} r \\ u \end{bmatrix}, \quad u = Ke. \tag{16}$$

Among them, the augmented object model is

$$G_H = \begin{bmatrix} W_1 & -W_1 G \\ 0 & W_2 \\ 0 & W_3 G \\ I & -G \end{bmatrix}. \tag{17}$$

It can be derived as

$$\psi = \begin{bmatrix} W_1 S \\ W_2 R \\ W_3 T \end{bmatrix} = \begin{bmatrix} W_1 \\ 0 \\ 0 \end{bmatrix} + \begin{bmatrix} -W_1 G \\ W_2 \\ W_3 G \end{bmatrix} K(I + GK)^{-1} = LFT(G_H(s), K(s)). \quad (18)$$

The right end of Equation (18) is the linear fraction transformation form of the objective function. Therefore, the problem of making the system internally stable and meeting the design index $\|\psi\|_\infty < 1$ of the controller $K(s)$ can be attributed to the design problem of increasing the H_∞ standard corresponding to the generalized controlled objects containing weighted functions $G_H(s)$. $G(s)$ is a model of a variable-thrust liquid rocket motor system under a particular operating condition.

2.3. Design of H-Infinity Mixed Sensitivity Controller. W_1 can take the diagonal real rational function matrix, the frequency domain width of low-frequency interference is w_1, and the influence of low-frequency interference on the system is attenuated by k_1 times. Determine w_c according to the requirements of the rocket engine response rapidity, make the amplitude-frequency characteristics of $W_1(j\omega) = k_1/(j\omega/\omega_1' + 1)$ exceed w_c [37], and select $W_1(j\omega)$ if it is satisfied (if not, increase the order of the controller).

W_2 represents the norm bound of the additive perturbation, which can be a diagonal real rational function matrix, and satisfies the restriction condition of formula $\bar{\sigma}[W_2^{-1}(j\omega)] \le \bar{\sigma}[G(j\omega)]$. In order not to increase the order of the controller, a constant real number is used, which means that the additive perturbation is a constant bound. Within a certain range, the larger the value, the smaller the $\|R\|_\infty$.

$W_3(j\omega)$ represents the norm bound of multiplicative perturbation. Therefore, $W_3(j\omega)$ should have high-pass properties. $W_3(j\omega)$ can be a diagonal nontrue rational function matrix. However, it must be ensured that $W_3(j\omega)G(j\omega)$ is a real rational function. So the number of times of the $W_3(j\omega)$ that the numerator is higher than the denominator is limited by this condition [38]. Subject to the restriction of $\bar{\sigma}[W_1^{-1}(j\omega)] + \bar{\sigma}[W_3^{-1}(j\omega)] \ge 1$, usually the frequency band of $W_3(j\omega)$ should be at the right end of, that is, the frequency bands of $W_1(j\omega)$ and $W_3(j\omega)$ do not overlap. For those with high-pass nature, the rising slope can be larger, for example, 40 dB per 10 octaves. As can be seen from the foregoing, the suppression of high-frequency interference by the closed-loop system can be ensured at this time.

Design the h-infinity controller for one of the working conditions of the variable-thrust liquid rocket engine, According to the above rules and based on the experiment method, the W_1, W_2, and W_3 can be obtained as

$$W_1 = \frac{s}{s + 0.0001s}, W_2 = 0.00001, W_3 = \frac{30s}{s + 500000s}. \quad (19)$$

The amplitude-frequency curves of $W_1(s)$ and $W_3(s)$ are shown in Figure 5. It can be found that the designed weight function satisfies the characteristics of $W_1(s)$ high-gain, low-pass, and $W_3(s)$ high-pass filtering well. Besides, the cut-off frequency of W_3 is higher than W_1.

Through the hinfsyn function in the MATLAB robust control toolbox, the form of robust controller can be obtained

$$K = \frac{\begin{array}{c} 8452s^{11} + 4.255e09s^{10} + 1.45e13s^9 \\ +2.948e16s^8 + 4.145e19s^7 + 4.29e22s^6 \\ +3.389e25s^5 + 2.011e28s^4 + 8.72e30s^3 \\ +2.553e33s^2 + 3.699e35s + 3.699e31 \end{array}}{\begin{array}{c} s^{12} + 9.755e06s^{11} + 5.22e10s^{10} + 1.389e14s^9 \\ +2.384e17s^8 + 2.896e20s^7 + 2.605e23s^6 \\ +1.725e26s^5 + 8.214e28s^4 + 2.593e31s^3 \\ +4.01e33s^2 + 8.019e29s + 7.612e25 \end{array}}. \quad (20)$$

Figure 6(a) shows the singular value curves of the sensitivity function $S(s)$ and $T(s)$ the weight function ${W_1}^{-1}(s)$, the penalty sensitivity function $T(s)$, and the weight function ${W_3}^{-1}(s)$ concerning ω, respectively.

$W_1 S$ represents the requirements for system tracking and interference suppression performance and should meet the necessary condition $\|W_1 S\|_\infty < 1\$, \$\bar{\sigma}[S(j\omega)] < \bar{\sigma}[{W_1}^{-1}(j\omega)]$; it can be seen from Figure 6(a) that the designed controller satisfies the systematic requirements. $W_3 T$ represents the requirement for the robust stability of the system, and the necessary condition of $\|W_3 T\|_\infty < 1$ should be satisfied, that is, to satisfy $\bar{\sigma}[T(j\omega)] < \bar{\sigma}[{W_3}^{-1}(j\omega)]$. As can be seen from Figure 6(b), it can be seen from the figure that the penalty sensitivity function is suppressed in the high-frequency band, and the designed controller meets the requirements of system performance.

As can be seen from Figure 7, the cutoff frequency of the system is $\omega_c = 103 rad/s$, and the phase margin is 72.6°. Therefore, the system is stable and has good robustness.

It can be seen from Figure 8 that the system has no overshoot after adopting h-infinity control, and the adjustment time is only 19 ms. After inputting constant value interference, it can recover quickly, and the steady-state error is close to 0. So when parameter uncertainty occurs, the engine can be quickly restored to condition.

2.4. ALQR Control Strategy

2.4.1. ALQR Control Principle. A linear quadratic regulator (LQR) is a feedback regulator that tries to ensure that each component of the system output vector or each component of the state vector is close to a balanced state when the system receives external force disturbances without consuming too many control resources. The LQR controller solves the minimum optimal regulation law $x(0) = x_0$ that satisfies the quadratic index under the condition of the initial state $u(t) = -kx(t)$.

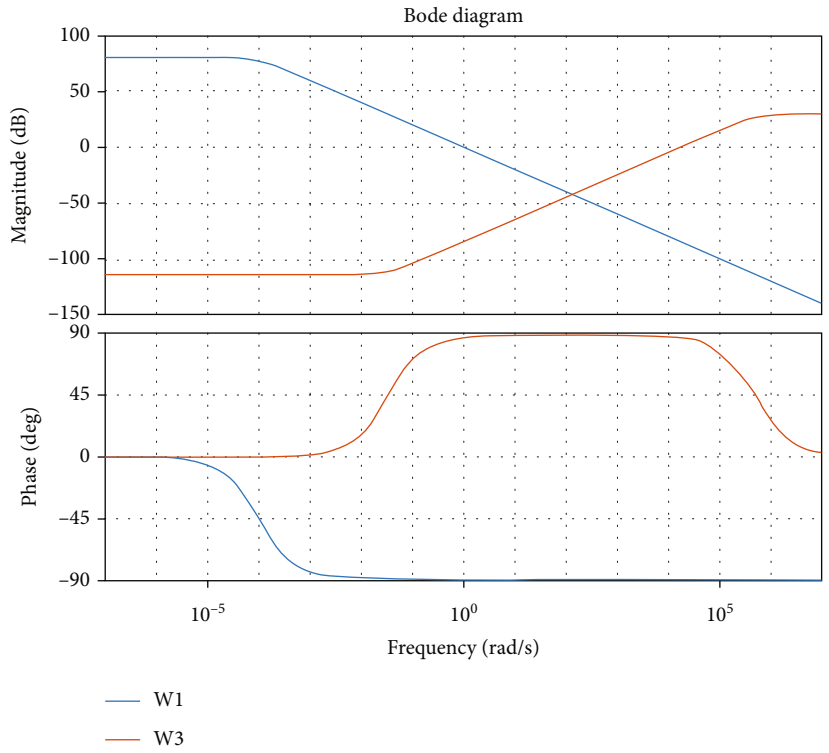

Figure 5: Amplitude-frequency curve of weight function $W_1(s)$ and $W_3(s)$.

$$J = \int_0^{\infty} \left[y^T(t) y(t) + u^T(t) R u(t) \right] dt. \tag{21}$$

Among them, Q is a symmetric nonnegative matrix, R is a symmetric positive definite matrix, and Q and R are called weight matrices. By choosing different weight matrices, the decay speed of the output represented by the index function J can be traded with the energy consumed by the control process [39]. That is, the control effect of the controller depends on the selection of the weight matrix. LQR is to solve the problem of state regulators and cannot meet the tracking control requirements of aeroengine commands. Therefore, in order to eliminate the steady-state error, an augmented method is used to introduce an integral link in each control loop of the design object model to form the internal model of the step input signal, which is the lowest common denominator of the unstable pole of the external input signal, reciprocal.

Describing the liquid rocket motor system in terms of state space yields $\begin{bmatrix} A & B \\ C & D \end{bmatrix}$. For the engine-controlled object containing the actuator, its mathematical model is a strictly regular system. In the system shown in Figure 9, $D = 0$ and the error e can be derived by deriving

$$\dot{e} = \frac{d(r - y)}{dt} = -\dot{y} = -C\dot{x}(t > 0). \tag{22}$$

The augmented state vector becomes $\bar{x} = \left[\dot{x}^T e^T \right]^T$. The design objects of the augmented LQR method are

$$\dot{\bar{x}} = \bar{A}\bar{x} + \bar{B}\bar{u}. \tag{23}$$

Among that $\bar{u} = \dot{u}$, $\bar{A} = \begin{bmatrix} A & 0 \\ -C & 0 \end{bmatrix}$, and $\bar{B} = \begin{bmatrix} B \\ 0 \end{bmatrix}$. Then design an LQR regulator for the system described by Equation (21), so that all state quantities are kept at zero: $\bar{x} = \left[\dot{x}^T e^T \right]^T = 0$. The original system state x remains unchanged and satisfies the requirement of no steady-state error. The augmented system performance functional is

$$\bar{A}^T P + P\bar{A} - P\bar{B}R^{-1}\bar{B}^T P + Q = 0. \tag{24}$$

Expressing $\bar{K}$ by $\dot{x}$ and e as a block matrix $\bar{K} = [K_{\dot{x}} K_E]$, we can get

$$\dot{u} = \bar{K}\bar{x} = [K_{\dot{x}} K_e] \begin{bmatrix} \dot{x} \\ e \end{bmatrix} = K_{\dot{x}}\dot{x} + K_e e. \tag{25}$$

To calculate the Laplace transform of Equation (25), the original system controller can be obtained as

$$u = K_{\dot{x}} x + \frac{K_e e}{s}. \tag{26}$$

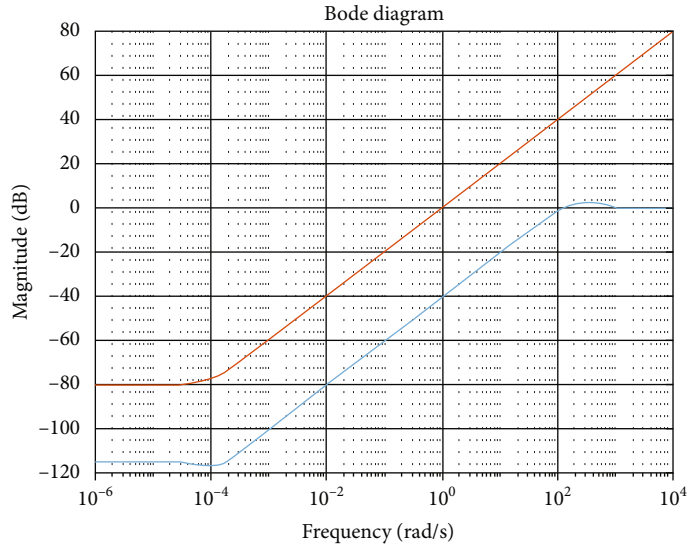

(a) The relationship between $S(s)$ and $W_1^{-1}(s)$

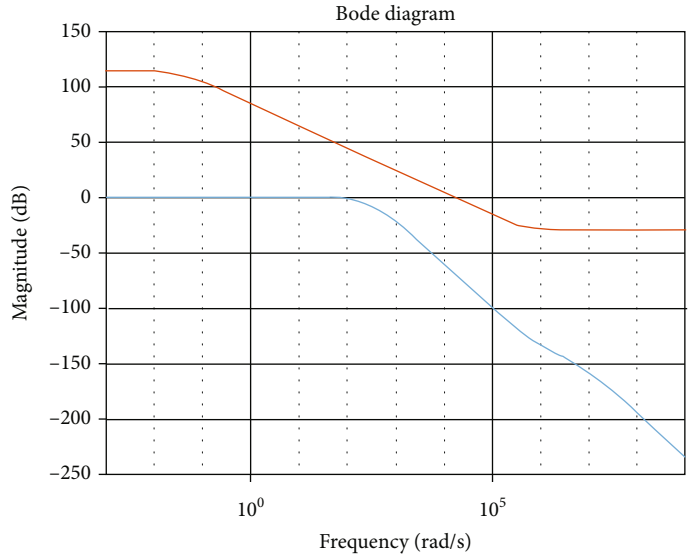

(b) The relationship between $T(s)$ and $W_3^{-1}(s)$

Figure 6: Singular value curve.

Select the same working condition of the variable-thrust liquid rocket engine to design the ALQR controller. According to the above method, the design object is augmented, and then, the LQR controller is obtained for the augmented design object [40]. You can get the ALQR controller

$$K_{\dot{x}} = [81.8737.7721.192],$$
$$K_e = 70.711. \quad (27)$$

Using the Simulink to simulate, the results are shown in Figure 10.

From Figure 10, the adjustment time is 17 ms when it receives external interference, and overshoot is only 2%. After inputting constant value interference, it can restore its own state, and the steady-state error tends to 0.

3. Result Comparison

The settling time of the two methods is similar, and the h-infinity method has a better response curve without

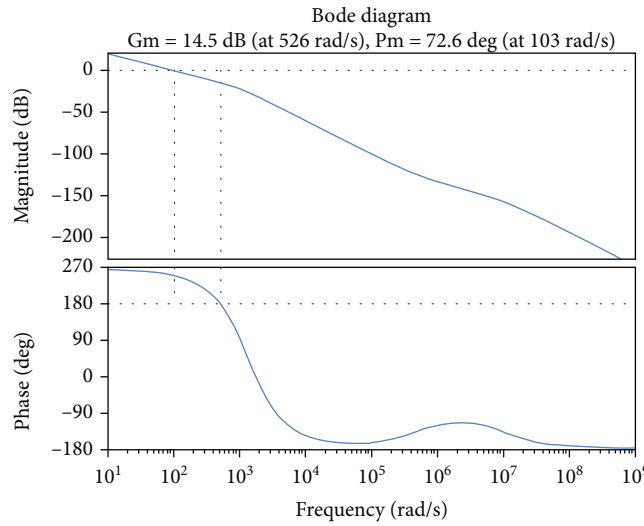

Figure 7: The open-loop transfer function curve of the system under H_∞ control.

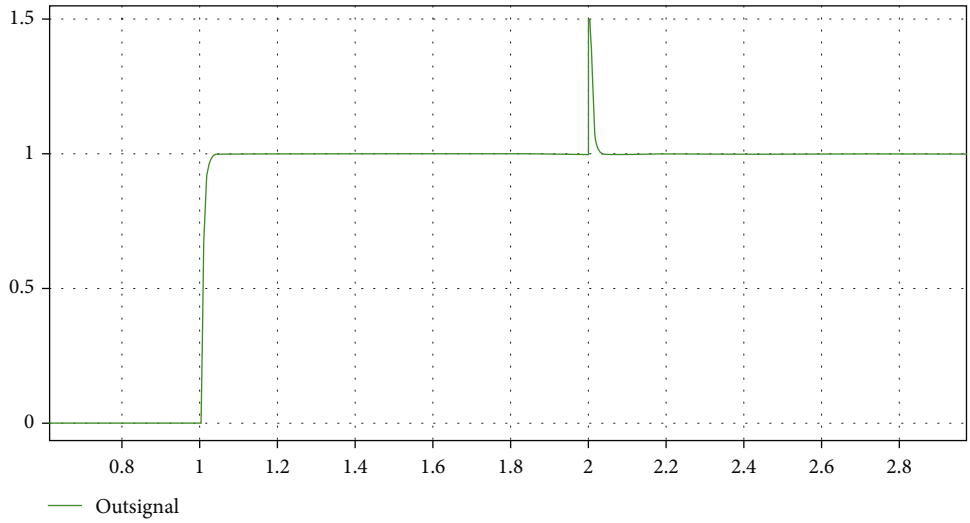

Figure 8: Step response and output under disturbance.

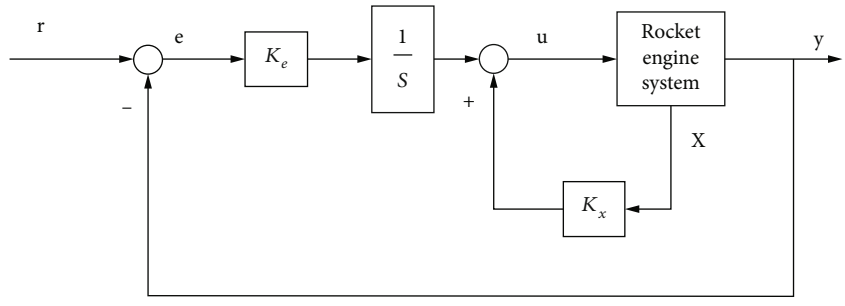

Figure 9: Augmented control system structure diagram.

overshoot. Aiming at the control stability of the large disturbance in the starting stage of the engine, a large-scale step signal is used to simulate the large disturbance in the starting stage. The state recovery curve of the control system is shown in Figure 11. The recovery time of the two systems is similar, and the h-infinite method of the recovery curve is superior. Based on the above control effects, the h-infinity controller is more complex in design than the ALQR

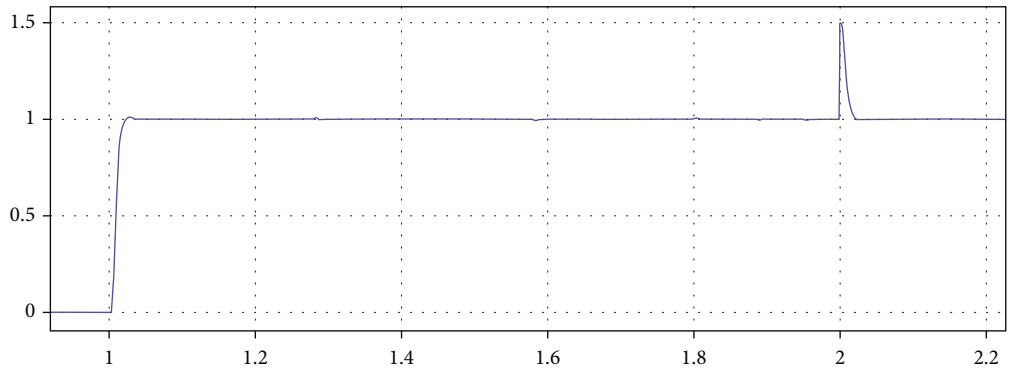

Figure 10: Step response and output under disturbance.

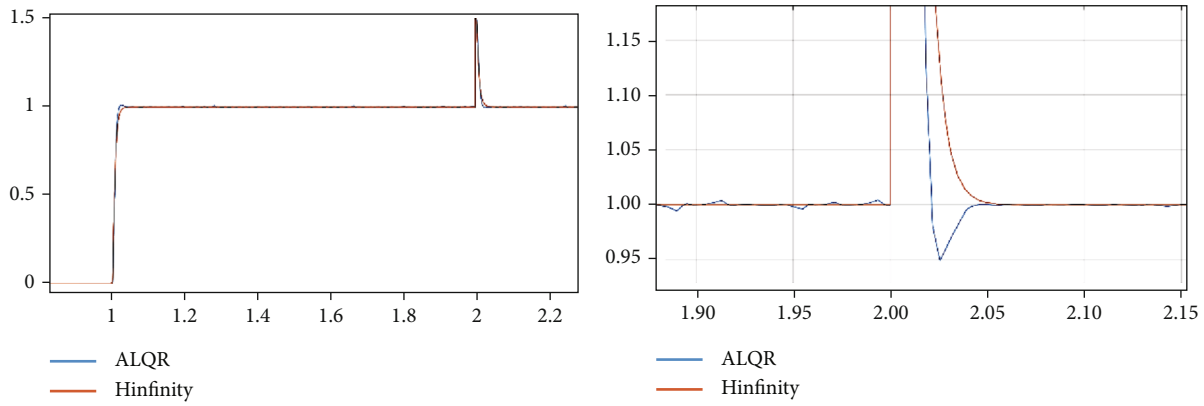

(a) Step response and output under disturbance

(b) Comparison of system state recovery under strong interference

Figure 11: System response curve.

controller, and the controller order is higher. Both control techniques used in this study are extremely robust. The h-infinity algorithm calculates the optimum $H\infty$-norm to generate a robust controller, which is then verified using Bode diagrams and single-condition simulation. It is possible to infer that the method described in this article is stable and efficient for the adaptive control algorithm framework. ALQR technology is based on the LQR method and is optimized for the control needs of engine command tracking. The steady-state error of the input signal is eliminated on the premise of ensuring its stability, and the performance in the simulation verification of a single working situation fulfills expectations.

4. Conclusions

A split-condition engine model is used to build a variable parameter robust controller that can continue to function successfully even when the operating conditions of the system are radically changed. This is based on the complicated operating situation of liquid rocket engines. To acquire the proper settings for each stage of the controller, we have embedded two various strong algorithms on this foundation.

The analysis of the simulation data reveals that both approaches can successfully track the step signal on the liquid rocket motor in steady-state without inaccuracy and without overshooting. Even if there is a disturbance signal, it is possible to quickly restore the system to its initial state. While the ALQR controller is more straightforward and has higher stability, the h-infinity controller is more robust and responds more quickly. Due to the experimental environment's limitations, the engine fitting model was used without more detailed modeling, and physical experiment verification has yet to be completed, making the integrity of the discussion in this paper somewhat regrettable. Furthermore, because there is currently no similar research, the simulation results lack horizontal comparison and analysis.

Data Availability

The simulation result data used to support the findings of this study are included within the article.

Conflicts of Interest

The authors declare that they have no conflicts of interest.

References

[1] S. Pérez-Roca, J. Marzat, H. Piet-Lahanier et al., "A survey of automatic control methods for liquid-propellant rocket engines," *Progress in Aerospace Sciences*, vol. 107, pp. 63–84, 2019.

[2] F. Xin, Z. Yulin, and C. Qizhi, "Pulse width sampled-data control for variable thrust liquid rocket engine[J]," *Journal of National University of Defense Technology*, no. 2, pp. 41–46, 1993.

[3] C. Yun-qin, "Variable gain solenoid valve control system used for hypergolic bipropellant variable thrust rocket engine," *Journal of National University of Defense Technology*, vol. 4, 1979.

[4] J. Bellows, R. Brewster, and E. Bekir, "Otv liquid rocket engine control and health monitoring," in *20th Joint Propulsion Conference*, p. 1286, Cincinnati,OH,U.S.A., 1984.

[5] S. Le Gonidec, "Method and a device for calculating a starting or stop sequence for an engine," US Patent 8, 364, 374, 2013.

[6] D. K. Huzel and D. H. Huang, "Chapter 7: Design of rocket-engine control and conditon-monitoring systems," *Modern Engineering for Design of Liquid-Propellant Rocket Engines, AIAA Progress in Astronautics and Aeronautics Richard Seebass*, 1992.

[7] Y. M. Timnat, *Advanced Chemical Rocket Propulsion*, Academic Press, 1987.

[8] C. F. Lorenzo and J. L. Musgrave, "Overview of rocket engine control," *AIP Conference Proceedings*, vol. 246, pp. 446–455, 1992.

[9] G. P. Sutton and O. Biblarz, *Rocket Propulsion Elements*, John Wiley & Sons, 2016.

[10] X. Dai and A. Ray, "Damage-mitigating control of a reusable rocket engine: part ii-formulation of an optimal policy," *Journal of Dynamic Systems, Measurement, and Control*, vol. 118, 1996.

[11] B. Kiforenko and A. Kharitonov, "Control of thrust of the liquid rocket engines: simulation and optimization," *Journal of Automation and Information Sci-ences*, vol. 32, no. 8, pp. 47–58, 2000.

[12] M. Klein, D. Hayoun, S. Le Gonidec, and S. Reichstadt, "Method and a circuit for regulating a rocket engine," US Patent App. 15/288, 521, 2017.

[13] E. W. Otto and R. A. Flage, *Control Of Combustion-Chamber Pressure and Oxidant-Fuel Ratio for a Regeneratively Cooled Hydrogen-Fluorine Rocket Engine*, National Aeronautics and Space Administration, 1959.

[14] H. Sunakawa, A. Kurosu, K. Okita, W. Sakai, S. Maeda, and A. Ogawara, "Automatic thrust and mixture ratio control of le-x," in *44th AIAA/ASME/SAE/ASEE Joint Propulsion Conference & Exhibit*, p. 4666, Hartford,CT, 2008.

[15] E. Nemeth, R. Anderson, J. Ols, and M. Olsasky, *Reusable rocket engine intelligent control system framework design*, NTRS - NASA Technical Reports Server, 1991, NASA CR 187213.

[16] S. Le Gonidec and O. Faye, "Device for adjusting an operating variable of an engine," US Patent 9,037,380, 2015.

[17] S. Le Gonidec, "Device for controlling a regulated system, and an engine 370 including such a device," US Patent 8,005,554, 2011.

[18] J. L. Musgrave, T.-H. Guo, E. Wong, and A. Duyar, "Real-time accommodation of actuator faults on a reusable rocket engine," *IEEE Transactions on Control Systems Technology*, vol. 5, no. 1, pp. 100–109, 1997.

[19] F. Zheng, M. Cheng, and W.-B. Gao, "Variable structure control of time-delay systems with a simulation study on stabilizing combustion in liquid propellant rocket motors," *Automatica*, vol. 31, no. 7, pp. 1031–1037, 1995.

[20] G. Zames, "On the input-output stability of time-varying nonlinear feedback systems–part II: conditions involving circles in the frequency plane and sector nonlinearities," *IEEE Transactions on Automatic Control*, vol. 11, no. 3, pp. 465–476, 1966.

[21] M. C. Tsai, E. J. M. Geddes, and I. Postlethwaite, "Pole-zero cancellations and closed-loop properties of an H^{∞} mixed sensitivity design problem," *Automatica*, vol. 28, no. 3, pp. 519–530, 1992.

[22] H. Kwakernaak, "Robust control and H_{∞}-optimization–tutorial paper," *Automatica*, vol. 29, no. 2, pp. 255–273, 1993.

[23] R. W. Beaven, M. T. Wright, and D. R. Seaward, "Weighting function selection in the H∞ design process," *Control Engineering Practice*, vol. 4, no. 5, pp. 625–633, 1996.

[24] G. Peng and X. Liyang, "Reliability analysis of multi-state systems based on improved universal generating function," *Acta Aeronauticaet Astronautica Sinica*, vol. 31, no. 5, pp. 934–939, 2010.

[25] E. Zafiriou, "Applied optimal control and estimation by Frank L. Lewis, prentice hall and texas instruments, englewood clgjs, nj, 1992,624 pp," *AICHE Journal*, vol. 40, no. 2, pp. 381-382, 1994.

[26] D. Miller and M. Rossi, "Simultaneous stabilization with near optimal LQR performance," *IEEE Transactions on Automatic Control*, vol. 46, no. 10, pp. 1543–1555, 2001.

[27] A. Ataei and Q. Wang, "Non-linear control of an uncertain hypersonic aircraft model using robust sum-of-squares method," *IET Control Theory & Applications*, vol. 6, no. 2, pp. 203–215, 2012.

[28] B. Bergeon, D. Martinez, P. Coustal, and J. Granier, "Design of an active suspension system for a micro-gravity experiment," *Control Engineering Practice*, vol. 4, no. 11, pp. 1491–1502, 1996.

[29] M. Lopez and F. Rubio, "H∞ multivariable design methodology for a ship," in *Procc. of 3rd European Control Conference*, pp. 607–612, Rome, Italy, 1995.

[30] H.-P. Lee and H.-Y. Hwang, "Design of two-degree-of-freedom robust controllers for a seeker scan loop system," *International Journal of Control*, vol. 66, no. 4, pp. 517–538, 1997.

[31] J. Yan and S. E. Salcudean, "Teleoperation controller design using H/sub ∞/-optimization with application to motion-scaling," *IEEE Transactions on Control Systems Technology*, vol. 4, no. 3, pp. 244–258, 1996.

[32] M. Ortega and F. Rubio, "Systematic design of weighting matrices for the H_{∞} mixed sensitivity problem," *Journal of Process Control*, vol. 14, no. 1, pp. 89–98, 2004.

[33] T. Fei, L. Yong, G. Yongbing, L. Wen, and W. Changjie, "On design and numerical simulation for linear throttling cavitation venturi," *Aerospace Control and Application*, vol. 39, pp. 12–16, 2013.

[34] H.-Z. Li, *Design of the Control System of a Variable Thrust Rocket Engine, [M.S. thesis]*, Northwestern Polytechnical University, 2005.

[35] C. F. Lorenzo, W. C. Merrill, J. L. Musgrave, and A. Ray, "Controls concepts for next generation reusable rocket engines," in *Proceedings of 1995 American Control Conference-ACC'95*, vol. 6, pp. 3942–3950, Seattle, WA, USA, 1995.

[36] Y.-X. Gao, P. Tian, and Q. Li, "Application of h\∞ mixed sensitivity control in main steam pressure system," *Proceedings of the Chinese Society of Universities for Electric Power System and Automation*, vol. 1, 2007.

[37] X. Wu and X. Xie, "Weighting function matrix selection in h robust control," *Journal-Tsinghua University*, vol. 37, pp. 27–30, 1997.

[38] M. G. Ortega, M. Vargas, F. Castaño, and F. R. Rubio, "Improved design of the weighting matrices for the s/ks/t mixed sensitivity problem-application to a multivariable thermodynamic system," *IEEE Transactions on Control Systems Technology*, vol. 14, no. 1, pp. 82–90, 2005.

[39] J.-C. Wang and Y.-Q. Guo, "Design of multi-variable augmented lqr controller for civil aero-engine," *Aeronautical Computing Technique*, vol. 5, 2014.

[40] Y. Gang and Y. Hua, "Choosing method for aeroengine lqr weighting," *Journal of Nanjing University of Aeronautics & Astronautics*, vol. 38, no. 4, 2006.